Bulletin of the Seismological Society of America, Vol. 102, No. 3, pp. 1214–1223, June 2012, doi: 10.1785/0120110183

Solving the Surface-Wave Eigenproblem with Chebyshev Spectral Collocation

by Marine A. Denolle, Eric M. Dunham, and Gregory C. Beroza

Abstract Stable and accurate surface-wave calculations present a long-standing numerical and analytical challenge to seismologists. In a layered medium, we can describe the surface-wave behavior with harmonic time dependence in terms of an eigenproblem where the eigenvalues and eigenfunctions define the surface-wave modes.

Numerous studies have explored diverse numerical approaches to solve this eigenproblem, but they tend to suffer from numerical difficulties that limit the complexity of the medium, frequency range of applicability, or accuracy of the solution. We propose an equivalent formulation that replaces the conventional stress-displacement vector with an alternative one, in order to cast the eigenproblem in a standard form that is linear in the eigenvalues. We discretize the system and boundary conditions using a Chebyshev spectral collocation method, leading to a finite-dimensional generalized matrix eigenvalue problem that can be solved directly. No iterations are required to satisfy the boundary conditions or to isolate the eigenmodes. Collocation methods allow for the solution of the eigenproblem for general depth-dependent elastic properties, including continuous depth variations of the properties as well as material interfaces. We illustrate the use of our technique to calculate dispersion curves, theoretical waveform time series, and to estimate the change from retrograde to prograde particle motion at the surface for a complex 1D structure under Los Angeles.

Introduction

Seismic waves in the Earth are modeled as elastic waves, and, to first order, the Earth can be approximated as a 1D medium because the depth variations of elastic properties are much stronger than the horizontal variations. In this study we focus on surface-wave solutions only. Neglecting lateral variations in material properties, in the absence of sources, the elastic wave equation in the frequency and horizontal-wavenumber domain takes the form of an eigenproblem. This problem has been solved by a variety of methods, beginning with the propagator-matrix approach of Thomson (1950) and Haskell (1953). The propagator-matrix technique begins with the assumption of a layered medium with spatially uniform elastic properties within each layer. The original method has been known to suffer from instabilities at high frequencies (Ewing *et al.*, 1957). Since these methods were introduced, seismologists have devised a number of approaches for obtaining accurate and stable solutions at high frequencies, including the delta matrix method (Pestel and Leckie, 1963; Watson, 1970;Buchen and Ben-Hador, 1996), the Schwab–Knopoff approach (Knopoff, 1964; Schwab and Knopoff, 1971), and the reflection and transmission (RT) matrix method (Kennett, 1974; Kennett and Clarke, 1979; Kennett, 2009; Pei *et al.*, 2008).

In addition to the propagator-matrix technique, the eigenvalue problem can also be solved using the shooting method. This is more accurate but can be computationally inefficient because it involves multiple iterations to satisfy all boundary conditions and to isolate particular eigenmodes (Takeuchi and Saito, 1972; Dahlen and Tromp, 1998). Another class of methods is based on directly approximating the eigenfunctions as a finite sum of polynomials or other special functions, with coefficients determined by minimizing appropriately defined residual functions. Galerkin finite element methods like those developed by Lysmer (1970) fall into this class, as do collocation methods. It is even possible to design hybrid methods that utilize both propagator-matrix and collocation techniques (Spudich and Ascher, 1983; Ascher and Spudich, 1986).

In this paper we focus on the surface-wave component of the seismic wave field and treat the coupled system of equations as an eigenproblem, where the eigenvalues (wavenumbers) and eigenfunctions comprise the surface-wave modes. We follow Kirrmann (1995) and recast the system of ordinary differential equations in the depth variable z into an equivalent linear eigenproblem in standard form

$$\mathbf{Lu} = k\mathbf{u} \tag{1}$$

for a wavenumber k and linear differential operator $\mathbf{L}$ involving d/dz and a frequency ω. The eigenvector $\mathbf{u}$ contains the displacement fields and certain components of the stress tensor as a function of depth z. The stress tensor components that enter $\mathbf{u}$ are different from those in the standard stress-displacement vector. The eigenproblem also requires appropriate boundary conditions.

We discretize the problem (1) by seeking values of $\mathbf{u}$ at a finite set of points, and convert the linear operator $\mathbf{L}$ into a matrix using a difference operator $\mathbf{D}$ to approximate the depth derivative d/dz. Boundary conditions are directly incorporated as constraint equations on the point values of $\mathbf{u}$ and $d\mathbf{u}/dz$ on the boundaries. This yields a generalized matrix eigenvalue problem

$$\mathbf{Au} = k\mathbf{Bu}, \tag{2}$$

where $\mathbf{A}$ and $\mathbf{B}$ involve $\mathbf{D}$ and are singular, preventing us from rewriting equation (2) as a standard eigenvalue problem. Numerical solution of the finite-dimensional eigenvalue problem is straightforward and directly yields all resolvable eigenmodes.

If we discretize this problem using N points with a standard finite-difference (FD) scheme, it converges for sufficiently smooth solutions with an error that decreases as N^{-p}, where p is the FD order of accuracy. We have found low-order FD methods to be computationally intensive, with unreasonably large values of N required for an accurate solution. Instead, we use a Chebyshev spectral collocation method that converges faster than N^{-p} for any p for smooth functions. Spectral accuracy is still possible in the presence of discontinuous material properties, provided the domain is split at material interfaces into multiple layers (within which properties are smoothly varying). Each layer is separately discretized, and fields on the two sides of the layer interface are coupled with appropriate continuity conditions.

We first show how to recast the eigenproblem in standard form. We then show that a spectral collocation discretization greatly improves the accuracy and efficiency relative to FD methods. We refer to this optimal combination as the generalized eigenproblem spectral collocation (GESC) method.

We verify the accuracy of our results against known analytical solutions for simple cases, and against well-established methods (Herrmann, 1978) for more complex media. Once verified, we apply our method to solve for the surface-wave response of the southern California crust as represented by a local profile of the Southern California Earthquake Center (SCEC) Community Velocity Model Version 4.0 (CVM4; Magistrale *et al.*, 2000; Kohler *et al.*, 2003). Our method is both efficient and general and does not suffer from instabilities at high frequencies. It is more flexible than other approaches because it allows for a combination of homogeneous layers, continuous gradients, discontinuities in material properties, and directly gives all surface-wave modes with no iterations needed to satisfy boundary conditions or to isolate particular modes.

Formulation of the Eigenproblem

We combine Hooke's law and the momentum balance for an elastic solid with depth-dependent properties to derive the eigenproblem in the Fourier domain. In cylindrical coordinates (r, ϕ, z), we seek a solution of the specific form (Aki and Richards, 2002)

$$\begin{aligned}\mathbf{u} = [&r_1(k,z,\omega)\mathbf{S}_k^m(r,\phi) + l_1(k,z,\omega)\mathbf{T}_k^m(r,\phi)\\ &+ ir_2(k,z,\omega)\mathbf{R}_k^m(r,\phi)]e^{-i\omega t},\end{aligned} \tag{3}$$

where $\mathbf{u}$ is the displacement field, z is the depth coordinate, ω is the frequency, and

$$\begin{aligned}\mathbf{T}_k^m(r,\phi) &= \frac{1}{kr}\frac{\partial Y_k^m}{\partial \phi}\mathbf{e}_r - \frac{1}{k}\frac{\partial Y_k^m}{\partial r}\mathbf{e}_\phi,\\ \mathbf{S}_k^m(r,\phi) &= \frac{1}{k}\frac{\partial Y_k^m}{\partial r}\mathbf{e}_\mathbf{r} + \frac{1}{kr}\frac{\partial Y_k^m}{\partial \phi}\mathbf{e}_\phi,\\ \mathbf{R}_k^m(r,\phi) &= -Y_k^m\mathbf{e}_z.\end{aligned} \tag{4}$$

The unit vectors of the cylindrical coordinate system are $(\mathbf{e}_r, \mathbf{e}_\phi, \mathbf{e}_z)$; the scalar displacement functions are $r_1(k,z,\omega)$, $l_1(k,z,\omega)$, and $r_2(k,z,\omega)$; and $Y_k^m(r,\phi) = J_m(kr)e^{im\phi}$, where m is the order of the Bessel function $J_m(\cdot)$ and k is the horizontal wavenumber. The elastic medium is characterized by its density ρ and Lamé parameters λ and μ. The compressional and shear wave speeds are α and β, respectively. The equations governing the Love and Rayleigh waves are

$$\begin{aligned}-\rho\omega^2 l_1 &= -\mu k^2 l_1 + \frac{d}{dz}\left(\mu\frac{dl_1}{dz}\right),\\ -\rho\omega^2 r_1 &= -k^2(\lambda+2\mu)r_1 - k\lambda\frac{dr_2}{dz}\\ &\quad + \frac{d}{dz}\left(\mu\frac{dr_1}{dz}\right) - k\frac{d}{dz}(\mu r_2),\\ -\rho\omega^2 r_2 &= k\mu\frac{dr_1}{dz} - k^2\mu r_2 + \frac{d}{dz}\left[(\lambda+2\mu)\frac{dr_2}{dz} + k\lambda r_1\right].\end{aligned} \tag{5}$$

The standard approach to solve equation (5) is to define the stress-displacement vectors for Love waves as (l_1, l_2), where $l_2 = \sigma_{z\phi}$, and for Rayleigh waves as (r_1, r_2, r_3, r_4), where $r_3 = \sigma_{rz}$ and $ir_4 = \sigma_{zz}$.

In this work, we assume a traction-free boundary condition at the free surface $z = 0$ and vanishing displacement at the bottom of the domain. The latter is known as the locked mode approximation in seismology (Harvey, 1981). Equation (5) yields the Love-wave eigenproblem

$$\frac{d}{dz}\begin{bmatrix} l_1 \\ l_2 \end{bmatrix} = \begin{bmatrix} 0 & \frac{1}{\mu} \\ k^2\mu - \rho\omega^2 & 0 \end{bmatrix}\begin{bmatrix} l_1 \\ l_2 \end{bmatrix}, \tag{6}$$

where $l_1 = 0$ at the bottom and $l_2 = 0$ at the free surface, and the Rayleigh-wave eigenproblem

$$\frac{d}{dz}\begin{bmatrix} r_1 \\ r_2 \\ r_3 \\ r_4 \end{bmatrix} = \begin{bmatrix} 0 & k & \frac{1}{\mu} & 0 \\ -k\frac{\lambda}{\lambda+2\mu} & 0 & 0 & \frac{1}{\lambda+2\mu} \\ k^2\frac{4\mu(\lambda+\mu)}{\lambda+2\mu} - \rho\omega^2 & 0 & 0 & k\frac{\lambda}{\lambda+2\mu} \\ 0 & -\omega^2\rho & -k & 0 \end{bmatrix}\begin{bmatrix} r_1 \\ r_2 \\ r_3 \\ r_4 \end{bmatrix}, \tag{7}$$

where $r_1 = r_2 = 0$ at the bottom and $r_3 = r_4 = 0$ at the free surface. The resulting system can be written as $d\mathbf{f}/dz = \mathbf{P}(z)\mathbf{f}(z)$, where $\mathbf{f}$ is the displacement-stress vector, and we can solve this boundary value problem either by direct integration from the bottom to the surface (Takeuchi and Saito, 1972) or by the propagator-matrix approach (Haskell, 1953). As written, the system is a quadratic rather than a linear eigenproblem, because k is raised to the second power.

We propose a reformulation of the surface-wave eigenproblem that offers advantages over the traditional approach described previously in this paper. We replace the stress functions l_2, r_3, and r_4 with

$$L_2 = k\mu l_1, \tag{8}$$

$$R_3 = k(\lambda + 2\mu)r_1 + \lambda\frac{dr_2}{dz}, \tag{9}$$

$$R_4 = \mu\frac{dr_1}{dz} - k\mu r_2, \tag{10}$$

respectively, where $\sigma_{r\phi} = iL_2$, and $\sigma_{rr} = iR_3$ and $R_4 = r_3 = \sigma_{rz}$.

The Love-wave eigenproblem becomes

$$\begin{bmatrix} 0 & \frac{1}{\mu} \\ \rho\omega^2 + \frac{d}{dz}\left(\mu\frac{d}{dz}\right) & 0 \end{bmatrix}\begin{bmatrix} l_1 \\ L_2 \end{bmatrix} = k\begin{bmatrix} l_1 \\ L_2 \end{bmatrix}, \tag{11}$$

where $l_1 = 0$ at the bottom and $\mu dl_1/dz = 0$ at the free surface. The Rayleigh-wave eigenproblem becomes

$$\begin{bmatrix} 0 & -\frac{\lambda}{\lambda+2\mu}\frac{d}{dz} & \frac{1}{\lambda+2\mu} & 0 \\ \frac{d}{dz} & 0 & 0 & -\frac{1}{\mu} \\ \rho\omega^2 & 0 & 0 & \frac{d}{dz} \\ 0 & -\rho\omega^2 - \frac{d}{dz}\left(\frac{4\mu(\lambda+\mu)}{\lambda+2\mu}\frac{d}{dz}\right) & -\frac{d}{dz}\frac{\lambda}{\lambda+2\mu} & 0 \end{bmatrix}\begin{bmatrix} r_1 \\ r_2 \\ R_3 \\ R_4 \end{bmatrix} = k\begin{bmatrix} r_1 \\ r_2 \\ R_3 \\ R_4 \end{bmatrix}, \tag{12}$$

where $r_1 = r_2 = 0$ at the bottom and $(\lambda + 2\mu)dr_2/dz + \lambda k r_1 = 0$ and $R_4 = 0$ at the free surface. If we include an internal layer interface, we must respect continuity of the displacements l_1, r_1, and r_2, and continuity of the traction components of stress $\mu dl_1/dz$, $(\lambda + 2\mu)dr_2/dz + \lambda k r_1$, and R_4.

Reduction to a Generalized Matrix Eigenvalue Problem

The left-hand sides of equations (11) and (12) involve linear operators with depth-dependent elastic parameters and spatial derivatives. We convert this to a finite-dimensional generalized matrix eigenvalue problem using a collocation method. We solve for the eigenfunctions at $N + 1$ collocation points within each layer (indexed by $i = 0, 1, \ldots, N-1, N$) by requiring that equations (11) and (12) be satisfied exactly at those points. We approximate d/dz with the $(N + 1) \times (N + 1)$ difference operator $\mathbf{D}$. For a field f with point values f_i, $(df/dz)_i = \sum_{j=0}^{N} D_{ij} f_j$.

To accommodate discontinuities in material properties, we layer the medium by placing internal interfaces at locations such that the eigenfunctions are smooth within the layers. Collocation points are placed on either side of an interface, and we enforce appropriate continuity conditions to relate fields on the two sides.

To incorporate the boundary and continuity conditions, we remove rows of the matrix system and replace them by appropriate equations of constraint. We illustrate the technique for Love waves in a single layer. We adopt the convention that z is positive downward with $z = 0$ being the free surface so that $i = 0$ is at the free surface and i increases with z until $i = N$ at the bottom. First, we discretize equation (11) as

$$\begin{bmatrix} \mathbf{0} & \boldsymbol{\mu}^{-1} \\ \mathbf{D}\boldsymbol{\mu}\mathbf{D} + \rho\omega^2 & \mathbf{0} \end{bmatrix}\begin{bmatrix} u_0^L \\ \vdots \\ u_{2N+1}^L \end{bmatrix} = k\begin{bmatrix} \mathbf{I} & \mathbf{0} \\ \mathbf{0} & \mathbf{I} \end{bmatrix}\begin{bmatrix} u_0^L \\ \vdots \\ u_{2N+1}^L \end{bmatrix}, \tag{13}$$

where $\mathbf{I}$ is the $(N + 1) \times (N + 1)$ identity matrix, the vector $\mathbf{u}^L$ contains the Love-wave displacement and stress $(\mathbf{l}_1 \quad \mathbf{L}_2)$ sampled at the collocation points, and $\boldsymbol{\mu}$ and $\boldsymbol{\rho}$ are diagonal matrices of the depth-dependent shear modulus and density, respectively, evaluated at the collocation points. The first $N + 1$ rows correspond to Hooke's law at the $N + 1$ collocation points, and the last $N + 1$ rows are the momentum balance equation at the same points.

To introduce the boundary conditions at the free surface and the bottom, we remove entire rows of the system and replace these with constraint equations. At the free surface $(i = 0)$, we replace Hooke's law with the condition $\mu_{00}\sum_{j=0}^{N} D_{0j}u_j^L = 0$, where μ_{00} is the first element of $\boldsymbol{\mu}$. This replaces the first row in equation (13). At the bottom $(i = N)$, we replace Hooke's law with the rigid-bottom condition $u_N^L = 0$. This replaces row $N + 1$ in equation (13). In

the more general case of a layered medium, coupling conditions at layer boundaries are incorporated using a similar approach. Once boundary conditions have been implemented, the resulting matrices **A** and **B** are singular, making this a generalized eigenvalue problem. The problem is readily solved using the QZ algorithm (Moler and Stewart, 1973), which is implemented in MATLAB's subroutine eig through an interface to the Linear Algebra PACKage (LAPACK) library.

Discretization Using a Chebyshev Collocation Method

The method described in the previous section can be implemented using any difference operator **D**. A simple approach would be to use a standard low-order FD approximation, for which the error would decrease as N^{-p} for some small integer p. Instead, we use a Chebyshev spectral collocation method. Spectral methods are by far the most efficient when the solution is smooth, in which case they converge faster than N^{-p} for any p. Chebyshev collocation methods are an appropriate choice for problems on a nonperiodic, bounded domain (Trefethen, 2000). The basic unknowns are the values of the fields at $N + 1$ collocation points. These values uniquely define a global degree N interpolation polynomial that can be used to evaluate the solution at any value of z. The interpolation polynomial can equivalently be written in terms of an expansion over the Chebyshev polynomials, but the method does not require solving for the coefficients of that expansion.

The collocation points are not evenly distributed over the interval; they are instead clustered near the boundaries. We first map the interval $z \in [a, b]$ to $\hat{z} \in [-1, 1]$ with the mapping $z = (a + b)/2 - \hat{z}(b - a)/2$. In this standard interval, the collocation points, $\hat{z}_n$, are the Chebyshev–Gauss–Lobatto points

$$\hat{z}_n = \cos\left(\frac{n\pi}{N}\right), \qquad n = 0, \ldots, N. \tag{14}$$

The differentiation matrix **D** for the Chebyshev method is well known, and the difference operation can be efficiently implemented with a fast Fourier transform (FFT) based algorithm (Trefethen, 2000).

Verification of the Numerical Method

In this section, we compare the Chebyshev collocation solution to solutions for simple models consisting of layers of constant elastic properties. This allows us to gauge how many points are needed within each layer to obtain a desired accuracy.

Single Layer Case

We first consider the simple case of a homogeneous finite-width layer with zero displacement at the bottom of the layer ($z = H$) and no traction at the surface ($z = 0$). The solutions for the fundamental and first four higher modes are shown in Figure 1 for both a second-order finite-difference discretization (FD2) and the Chebyshev spectral discretization (GESC). The two methods find the correct solution for the fundamental mode; however, the spectral approach is much more accurate for a given number of points, and for the number of points (~50) used in the FD2 approach, the solution was very inaccurate for higher modes. Note the dramatic difference in the convergence rate between the two methods. Even 100 points do not provide enough resolution to accurately recover the higher modes with the low-order FD approach.

Multilayer Case

Next we consider the multilayer case with discontinuities in elastic properties across horizontal interfaces. Analytical solutions become algebraically awkward for multiple layers, so we compare our results with eigenfunctions generated from a widely known and verified algorithm Computer Programs in Seismology (Herrmann, 1978), which we refer to as CPS. Those solutions are calculated using the Haskell–Thomson propagator-matrix technique that includes a bottom boundary condition for the semi-infinite half-space. To approximate this condition, we add a thick layer at the bottom of our model. We find that for a fixed frequency, a layer with $\omega H/\beta > 10$ provides a satisfactory approximation (error $< 10^{-10}$) to the half-space. As a test case, we use a medium with four homogeneous layers over a thick layer that approximates an underlying half-space (Table 1).

As shown in Figure 2, for periods of 1 and 3 s, both methods accurately retrieve the displacement eigenfunctions for the four first modes. In this case, the size of the residuals depends not only on the accuracy of our solution but also on the accuracy of the propagator technique and the degree to which our lowermost layer approximates a half-space. Figure 2 verifies that the two techniques provide the same solution for both Love and Rayleigh waves for all four modes at both periods considered.

Stability, Accuracy, and Efficiency

In the original propagator-matrix methods, numerical instabilities arose at high frequencies due to the inexact cancellation of extremely large terms (the exponentially growing solutions of the elastic wave equation) of opposite sign. The collocation method completely avoids this because exponentially growing functions are never evaluated, and the method is therefore free of instability even at high frequencies. Of course, obtaining an accurate solution requires using enough points to resolve the spatial variation of the eigenfunctions, and this increases the size of the matrix system. Consequently, it is unavoidable that the computational expense increases if one seeks to accurately solve for the high-order modes at high frequencies.

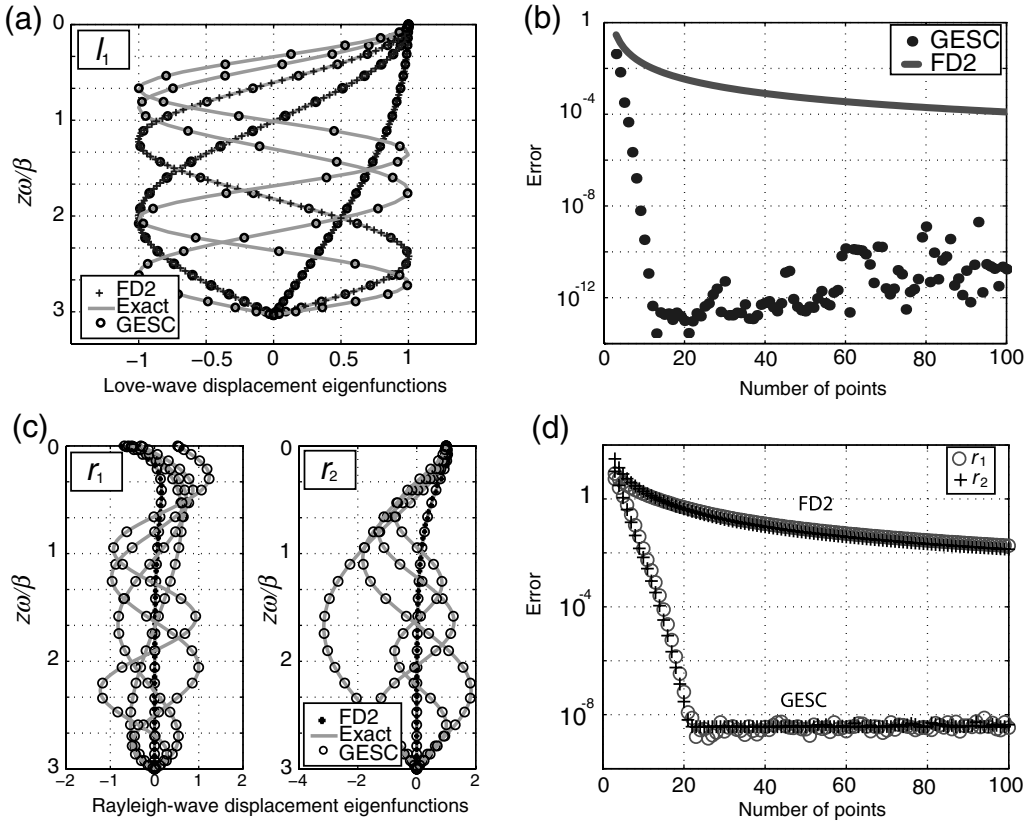

Figure 1. Surface-wave eigenfunctions for a single homogeneous layer with $\omega H/\beta = 3$. (a) Love-wave displacement eigenfunctions l_1 for the first five modes. (b) L_∞ error between the Love-wave numerical and exact solutions for the fundamental mode. GESC agrees to within machine precision after only 12–16 points, while the FD2 method converges much more slowly. (c) Rayleigh-wave horizontal (r_1) and vertical (r_2) displacement eigenfunctions for the first five modes. (d) L_∞ error between the Rayleigh-wave numerical and exact solutions for the fundamental mode.

Using a spectral method as opposed to a low-order FD or finite element method minimizes the number of points required for accuracy, as demonstrated by the examples shown previously in this paper. Further increases in efficiency are possible by employing an adaptive sampling strategy that adds resolution only where eigenfunction variations are likely to be strongest (e.g., near the free surface or material interfaces).

We illustrate this by solving for the fundamental mode at high frequencies (1–50 Hz) using two sampling strategies. To quantify the efficiency, we determine the minimum number of grid points required to reach a given accuracy measured in terms of the L_2 norm of the difference between our solution and a high resolution reference solution. We refine the mesh until the error drops below a given tolerance (i.e., 10^{-3} or 10^{-6}). We focus on the specific material structure shown in Figure 3a, which consists of three layers. The uppermost layer, of thickness H, has an average shear wave speed β_0.

Table 1
Elastic Properties in the Layered Medium

Layer Base (km)	ρ (kg/m^3)	β (km/s)	α (km/s)
12.5	2400	3	5.19
25	2625	3.5	6.06
37.5	2850	4	6.93
50	3075	4.5	7.79
1000	3300	5	8.66

One sampling strategy (not adaptive) is to increase the number of points, or resolution, in the first layer until meeting the accuracy criterion. The second strategy (adaptive) is to divide the first layer into two layers, with the shallowest having a frequency-dependent thickness $H_1 = \beta_0 T/2$ and the second layer having a thickness $H_2 = H - \beta_0 T/2$, where T is the period. We then only refine within the upper layer. This allows us to preserve high resolution near the surface where the spatial variations of the fundamental mode eigenfunctions are strongest while avoiding unnecessary refinement at greater depths where the eigenfunctions either vary slowly or have negligible amplitude. The choice $\beta_0 T/2$ may not be optimal, but it suffices for this comparison.

In Figure 3b, we display the number of points required to reach a desired accuracy as the frequency increases. In the first case (not adaptive), the required number of points monotonically increases with frequency and the method becomes computationally inefficient. In the second case (adaptive), the required number of points levels off and it

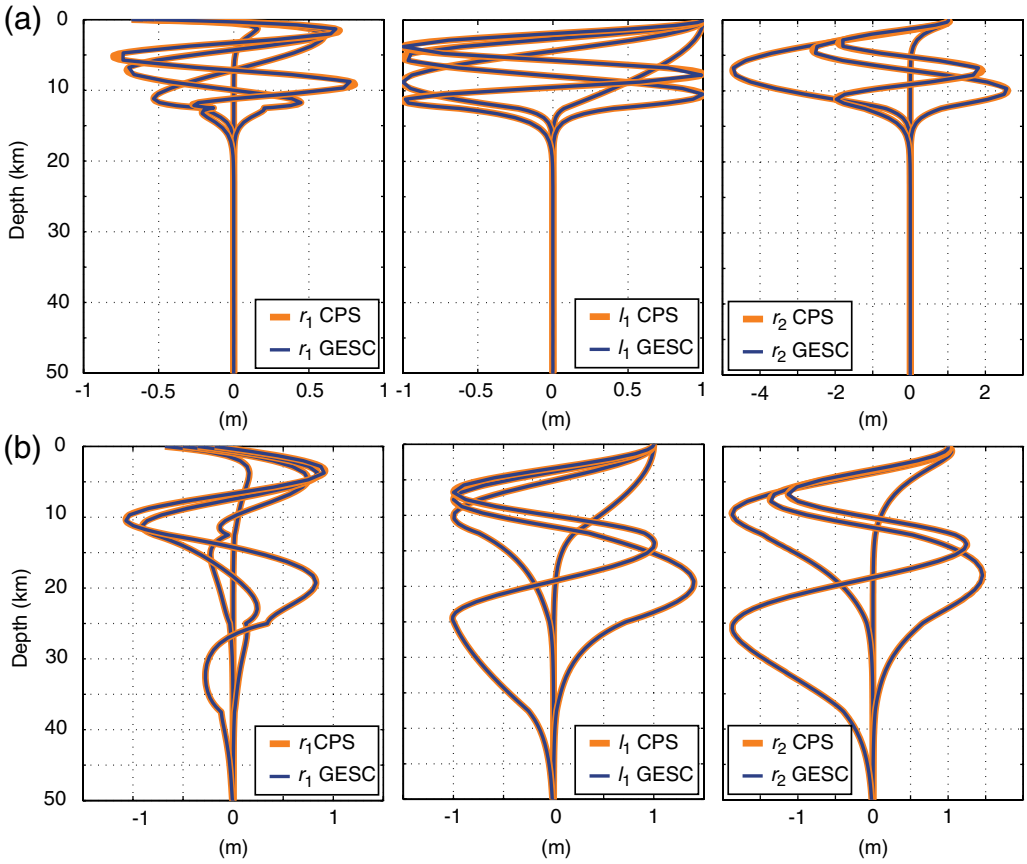

Figure 2. Comparison of the CPS and GESC solutions for the fundamental and first three higher mode surface-wave displacement eigenfunctions (l_1, r_1, and r_2) for (a) $T = 1$ s and (b) $T = 3$ s in a layered medium (see Table 1). The color version of this figure is available only in the electronic edition.

is possible to achieve a desired accuracy at arbitrarily high frequencies without increasing the overall number of points. This simple test reveals the advantage of using an adaptive sampling strategy to minimize computational expense. One can envision a procedure that automatically adjusts the number of points in each layer, or even the number of layers, to maximize efficiency, but we have not pursued this.

Now we have verified our technique for single and multilayer cases, primarily for cases with constant properties in each layer. The power of the collocation approach becomes more evident when there are gradients in the elastic properties. In this case, the propagator-matrix technique loses accuracy because it replaces a medium of continuously varying properties with a stack of homogeneous layers. In the

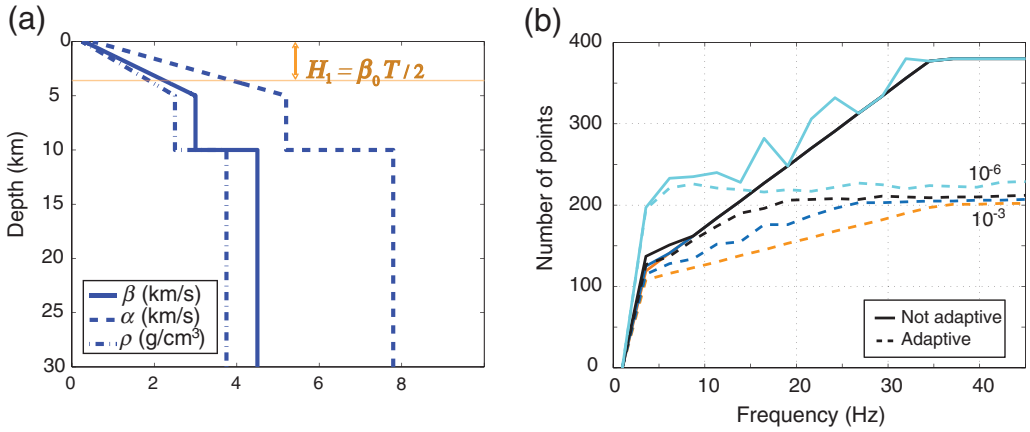

Figure 3. (a) Velocity profile used, where H_1 is the frequency-dependent thickness for the adaptive sampling. (b) Number of points required to achieve the accuracy level given in the legend, as a function of frequency for the fundamental mode solution. Solid lines show the original sampling, and dashed lines show the adaptive sampling The color version of this figure is available only in the electronic edition.

following sections, we solve the eigenproblem for complex velocity structures, including an example featuring thick sedimentary layers in a deep sedimentary basin. We illustrate the technique by extracting dispersion curves for a 1D profile from the Los Angeles basin, which is an exceptionally deep (9 km) basin that is likely to have very complex surface-wave modes. We take our velocity profiles from the SCEC CVM4 (Magistrale *et al.*, 2000; Kohler *et al.*, 2003).

Dispersion Curves

Surface-wave tomography depends on dispersion, as expressed by variations in the phase velocity c and group velocity U with frequency. These can be related using the energy integrals

$$c_R = \frac{\omega}{k_R}, \qquad c_L = \frac{\omega}{k_L}, \qquad U_R = \frac{I_2^R + I_3^R/(2k_R)}{c_R I_1^R},$$
$$U_L = \frac{I_2}{c_L I_1}, \tag{15}$$

where for Love waves

$$I_1^L = \frac{1}{2}\int_0^\infty \rho l_1^2\, dz, \qquad I_2^L = \frac{1}{2}\int_0^\infty \mu l_1^2\, dz, \tag{16}$$

and for Rayleigh waves

$$I_1^R = \frac{1}{2}\int_0^\infty \rho(r_1^2 + r_2^2)\, dz,$$
$$I_2^R = \frac{1}{2}\int_0^\infty [(\lambda + 2\mu) r_1^2 + \mu r_2^2]\, dz,$$
$$I_3^R = \frac{1}{2}\int_0^\infty \left[\lambda r_1 \frac{dr_2}{dz} - \mu r_2 \frac{dr_1}{dz}\right] dz. \tag{17}$$

The eigenfunctions are known at the Chebyshev collocation points, providing a unique polynomial representation of the solution. We use the Clenshaw–Curtis quadrature to evaluate the energy integrals by simply calculating the dot product of the energy integrands at the collocation points and the quadrature weights (Trefethen, 2000, ch. 12).

In Figure 4, we verify the accuracy of the dispersion curves by comparing our results with the dispersion curves calculated with CPS. This demonstrates the accuracy and efficiency of the Chebyshev spectral collocation method for surface-wave eigenfunctions, wavenumbers, and dispersion curves. Thus, we have at hand all of the tools necessary to generate synthetic surface-wave waveforms.

Time Domain Waveforms

We seek to generate theoretical waveforms for surface waves in the far-field limit. We follow Aki and Richards (2002, ch. 7, eqs. 7.148, 7.150, and 7.151) and express the displacement fields for surface waves generated by a point moment tensor source at depth h recorded at distance r and azimuth ϕ in terms of the eigenfunctions.

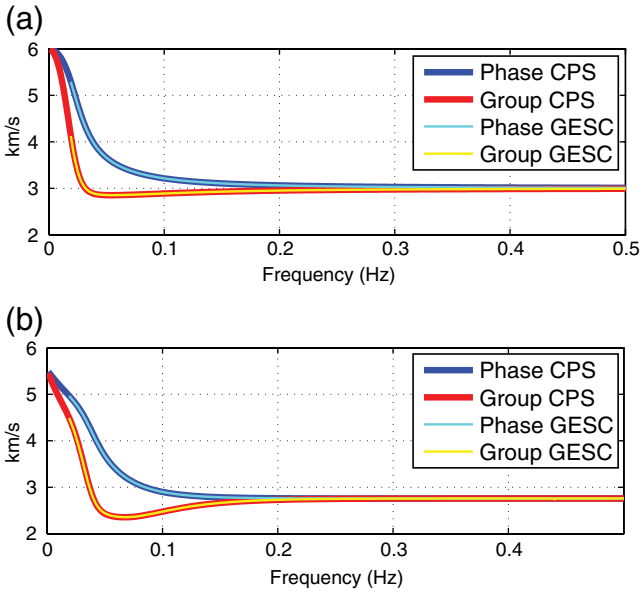

Figure 4. Comparison between dispersion curves of phase velocity (top curve) and group velocity (bottom curve) for CPS and GESC solutions for fundamental mode (a) Love and (b) Rayleigh waves. Because of the finiteness of our bottom layer, we do not compare the very low frequency solutions. The color version of this figure is available only in the electronic edition.

We build a layered model (see Table 1) with constant properties in each layer for this test case. We use a parabolic moment-rate function (Herrmann, 1978) with the Fourier spectrum

$$\dot{M}_0(\omega) \propto \exp(-i\omega 2\tau)\frac{4\sin^2(\omega\tau/2)\sin(\omega\tau)}{(\omega\tau)^3}, \tag{18}$$

where τ is the width of the parabola in time. We compute the spectrum of the surface-wave displacements at each frequency, given a frequency sampling that depends on the time sampling and length of the time series of interest. In the following example, we generate a time series of 1000 s and 4096 points using the FFT, which leads to $\Delta t = 0.24$ s.

In Figure 5, we compare results from the two methods for a double couple source for a moderate earthquake in southern California (based on the 8 December 2008 M 5.4 Chino Hills event, with strike 291°, rake 142°, dip 58°, and scalar moment $M_0 = 1.53 \times 10^{17}$ N·m). The moment tensor is provided by the Southern California Earthquake Data Center and involves both strike-slip and thrust components. We impose the source at 5 km depth and compute the displacement fields for a surface receiver at a distance of 300 km and an azimuth of 50°.

The waveforms clearly overlap, which verifies our method for the far-field case. As mentioned earlier, the power of the spectral approach is that it allows for a general variation of properties with depth.

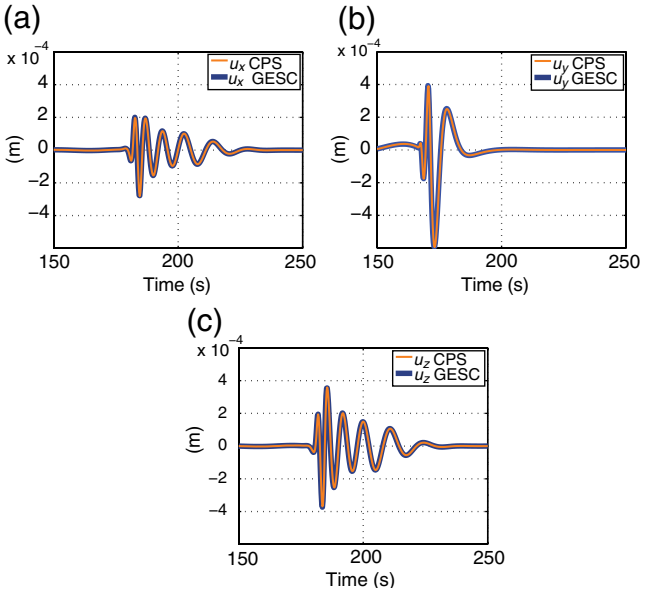

Figure 5. Comparison between the results from GESC and the waveforms obtained using the CPS technique. The color version of this figure is available only in the electronic edition.

Two Examples for Southern California

To demonstrate the technique, we apply it to 1D profiles of the 3D SCEC CVM4 for the southern California crust and upper mantle at several locations of interest. The model has a combination of layers, gradients, and large discontinuities, which are straightforward to incorporate in our approach.

The first case we consider is the change in retrograde to prograde particle motion of the Rayleigh fundamental mode that can occur when sediments overlie hard bedrock. Tanimoto and Rivera (2005) suggest that the presence of very low shear wave speed at the surface could change the Rayleigh wave particle motion from retrograde to prograde, and, for the special case of the Los Angeles sedimentary basin, this reversal lies in the frequency band of 0.06–0.17 Hz depending on the thickness of the sedimentary layer. We investigate these findings, first with an idealized velocity model used by Tanimoto and Rivera (2005).

We obtain the same transitions between retrograde and prograde motion for those cases, as highlighted by the gray box in Figure 6. The lower the surface shear velocity is, for a sediment thickness, the more likely prograde particle motion becomes. We next consider 1D velocity profiles under several seismic stations located above the thickest parts of the Los Angeles sedimentary basin. In Figure 7 we display the ratio of the horizontal and vertical eigenfunctions at the Earth's surface. While we do not see any changes in the sense of particle motion at locations near the deepest part of the sedimentary basin (WTT, USC, LGB, and LLS), there are interesting changes in behavior with the surface shear velocity showing $u_x(0)$ almost four times as large as $u_z(0)$. Tanimoto and Rivera (2005) argue that this corresponds to the resonant period of the sedimentary layer for vertically traveling shear waves. It is interesting to note that, in this case, the 5–8 s periods we find are similar to the resonant frequency of the geometry of the basin and the 1D structure. Surprisingly, the change from retrograde to prograde particle motion occurs at a shallower part of the sedimentary basin at CHN. At this location, the sediments are thinner and the gradient in the elastic parameters is much stronger, which results in the change in particle motion.

The second case we consider is Chino Hills, which was the site of a modest M 5.4 earthquake in July 2008 that occurred at 12.4 km depth. Although we cannot reproduce 3D effects from the sedimentary basin in our simulations, we can demonstrate the effect of depth on surface-wave excitation for this source. This is important because the Puente Hills Thrust, which underlies the basin, has the potential for large earthquakes that could strongly excite basin resonances. We explore what would be the impact of a deep versus shallow source on the theoretical displacement spectra at a distant

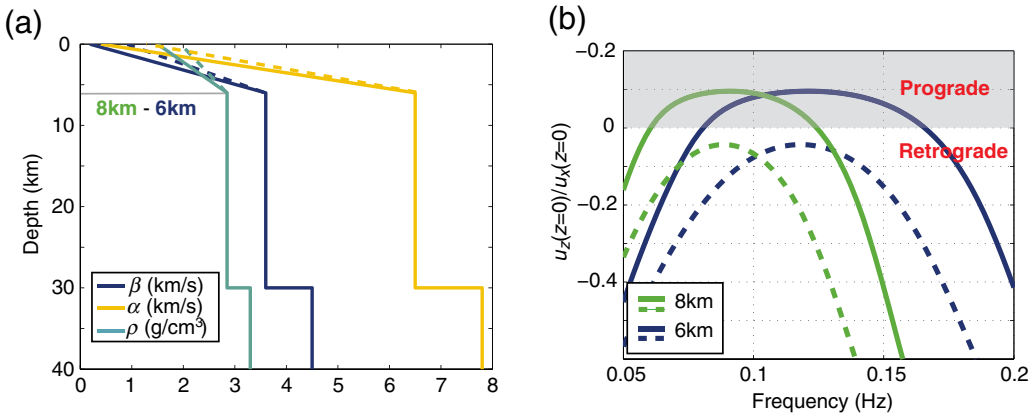

Figure 6. (a) Idealized velocity structure with thick sedimentary layers (6 and 8 km). (b) Changes from retrograde to prograde motion for Rayleigh waves as indicated by the ratio $u_z(0)/u_x(0)$. For a given sediment thickness, we see a change in retrograde to prograde motion from 0.07 to 0.18 Hz (for 6-km-thick sediments) and from 0.06 to 0.12 Hz (for 8-km-thick sediments), highlighted in gray, given the surface shear velocities $\beta_0 = 0.1605$ km/s (solid lines) and $2\beta_0$ (dashed lines). The color version of this figure is available only in the electronic edition.

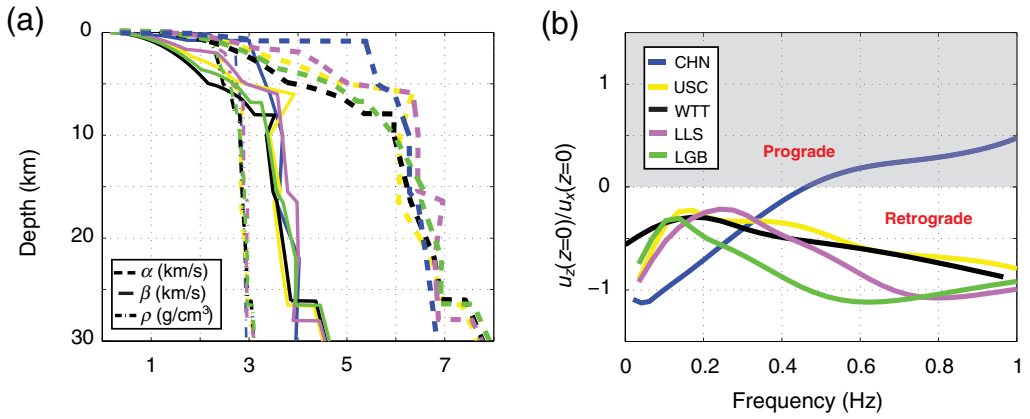

Figure 7. (a) Velocity structure in the Los Angeles area interpolated from CVM4. (b) $u_z(0)/u_x(0)$ as a function of frequency. We do not see changes in Rayleigh-wave polarization for the locations in the deepest part of the sedimentary basin, but we do see the retrograde to prograde transition occurring at higher frequency for CHN. The color version of this figure is available only in the electronic edition.

station (SDD) in Orange County, for sources in the sediments at depths of 4 and 8 km, and at 13 km depth in the underlying bedrock, near the site of the Chino Hills earthquake. In the time series, we impose a moment-rate function with a width of $\tau = 0.5$ s as in equation (18).

As expected in Figure 8, the depth of the source in this particular velocity profile strongly influences the wave excitation. For the shallow source (4 km), high frequency surface waves are much more strongly excited. The velocity structure and the depth of the source have a strong effect on the resulting ground motion predicted in terms of duration and spectrum of the shaking.

Conclusions

We have developed a formulation of the surface-wave eigenproblem in standard linear form and converted it to a generalized matrix eigenvalue problem using a Chebyshev spectral collocation method. The spectral collocation approach allows us to solve the eigenproblem with high accuracy using a minimal number of points per layer (generally about 20–30 for fundamental mode calculations). The accuracy of spectral methods makes this technique highly efficient. We verified the method by testing our results against analytical solutions for simple velocity structures and

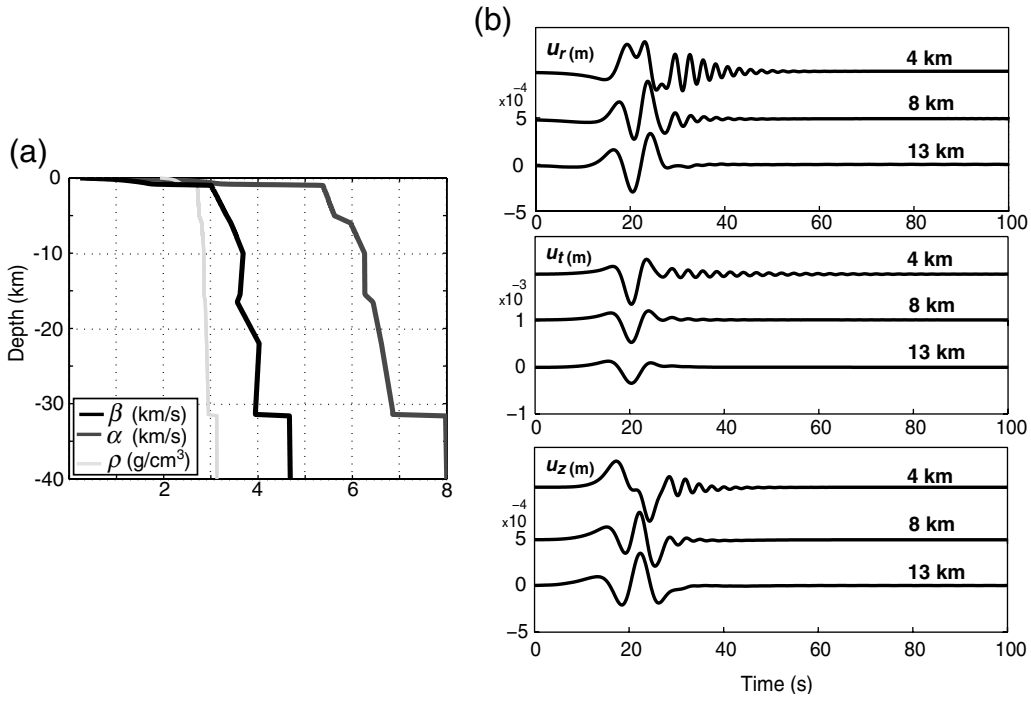

Figure 8. (a) Velocity structure under CHN seismic station (SCEC CVM4). (b) Displacement time series expected at SDD for the Chino Hills source described in the paper.

against solutions calculated with traditional methods (Herrmann 1978) for more complex structures.

We have not considered anelasticity in this study. In similar formulations, anelastic effects of a linear viscoelastic solid can be incorporated by allowing the elastic moduli to assume complex, frequency-dependent values. Although we have not implemented it, this approach should be straightforward to handle in our method because the eigenvalue solver can also be effectively applied to complex matrix systems having complex eigenvalues.

The power of using spectral collocation methods for this eigenproblem is that they permit general variations of properties with depth and solve the eigenproblem in an accurate and efficient manner. This allows for the type of complexities in shallow crustal structure (sediment consolidation with depth, sharp interfaces, and low velocity zones) that we expect to encounter in practical situations. The frequency range that can be solved is broad, and our technique is free of numerical difficulties at high frequencies, provided we optimize the number of points in each layer to ensure adequate resolution and minimize the total number of points used.

We demonstrated the utility of our method by calculating dispersion curves and theoretical surface-wave seismograms in the far-field approximation. We applied the method to particular locations from the Los Angeles sedimentary basin. We did not find the retrograde to prograde particle motion switch at the specific locations of the SCEC CVM4 mentioned by Tanimoto and Rivera (2005); however, we did see it at locations where the sedimentary basin is shallow and where the gradient with depth of the elastic parameters is very strong.

Data and Resources

The velocity profiles in Los Angeles were extracted from the Southern California Earthquake Data Center.

Acknowledgments

We thank Robert Herrmann for helpful discussions. This work was supported by NSF Grant EAR-0943885. This research was also supported by the Southern California Earthquake Center (SCEC). SCEC is funded by NSF Cooperative Agreement EAR-0529922 and USGS Cooperative Agreement 07HQAG0008. The SCEC contribution number for this paper is 1506.

References

Aki, K., and P. G. Richards (2002). *Quantitative Seismology*, Second Ed., University Science Books, Sausalito, California, 700 pp.

Ascher, U., and P. Spudich (1986). A hybrid collocation method for calculating complete theoretical seismograms in vertically varying media, *Geophys. J. Roy. Astron. Soc.* **86,** 19–40.

Buchen, P. W., and R. Ben-Hador (1996). Free-mode surface-wave computations, *Geophys. J. Int.* **124,** 869–887.

Dahlen, F. A., and J. Tromp (1998). *Theoretical Global Seismology*, Princeton University Press, Princeton, New Jersey, 944 pp.

Ewing, M., W. S. Jardetzky, and F. Press (1957). *Elastic Waves in Layered Media*, McGraw-Hill, New York, 380 pp.

Harvey, D. J. (1981). Seismogram synthesis using normal mode superposition: The locked mode approximation, *Geophys. J. Roy. Astron. Soc.* **66,** 37–69.

Haskell, N. A. (1953). The dispersion of surface waves on multilayered media, *Bull. Seismol. Soc. Am.* **43,** 17–34.

Herrmann, R. B. (1978). Computer Programs in Earthquake Seismology, Volume 2: General Programs, *Techical Report*, Saint Louis University.

Kennett, B. L. N. (1974). Reflections, rays, and reverberations, *Bull. Seismol. Soc. Am.* **64,** no. 6, 1685–1696.

Kennett, B. L. N. (2009). *Seismic Wave Propagation in Stratified Media*, The Australian National University, Canberra, Australia, 497 pp.

Kennett, B. L. N., and T. J. Clarke (1979). Seismic waves in a stratified half space, *Geophys. J. Roy. Astron. Soc.* **57,** 557–583.

Kirrmann, P. (1995). On the completeness of Lamb modes, *J. Elasticity* **37,** 36–39.

Knopoff, L. (1964). A matrix method for elastic wave problems, *Bull. Seismol. Soc. Am.* **54,** no. 1, 431–438.

Kohler, M. D., H. Magistrale, and R. W. Clayton (2003). Mantle heterogeneities and the SCEC reference three-dimensional seismic velocity model version 3, *Bull. Seismol. Soc. Am.* **93,** no. 2, 757–774.

Lysmer, J. (1970). Lumped mass method for Rayleigh waves, *Bull. Seismol. Soc. Am.* **60,** no. 1, 89–104.

Magistrale, H., S. Day, R. W. Clayton, and R. Graves (2000). The SCEC southern California reference three-dimensional seismic velocity model version 2, *Bull. Seismol. Soc. Am.* **90,** no. 6B, S65–S76.

Moler, C. B., and G. W. Stewart (1973). An algorithm for generalized matrix eigenvalue problems, *SIAM J. Numer. Anal.* **10,** no. 2, 241–256.

Pei, D., J. N. Louie, and S. K. Pullammanappallil (2008). Improvements on computation of phase velocities of Rayleigh waves based on the generalized R/T coefficient methods, *Bull. Seismol. Soc. Am.* **98,** no 1, 280–287.

Pestel, E. C., and F. A. Leckie (1963). *Matrix-Methods in Elasto-Mechanics*, McGraw-Hill, New York, 453 pp.

Schwab, F., and L. Knopoff (1971). Surface waves on multilayered anelastic media, *Bull. Seismol. Soc. Am.* **61,** no. 4, 893–912.

Spudich, P., and U. Ascher (1983). Calculation of complete theoretical seismograms in vertically varying media using collocation methods, *Geophys. J. Roy. Astron. Soc.* **75,** 101–124.

Takeuchi, H., and N. Saito (1972). Seismic surface waves, in *Methods in Computational Physics*, B. A. Bolt (Editor), Academic Press, New York, 217–295.

Tanimoto, T., and L. Rivera (2005). Prograde Rayleigh wave particle motion, *Geophys. J. Int.* **162,** 399–405.

Thomson, W. T. (1950). Transmission of elastic waves through a stratified solid medium, *J. Appl. Phys.* **21,** 89–93.

Trefethen, L. N. (2000). *Spectral Methods in MATLAB*, Society of Industrial and Applied Mathematics, Philadelphia, 165 pp.

Watson, T. H. (1970). A note on fast computation of Rayleigh wave dispersion in the multilayered half-space, *Bull. Seismol. Soc. Am.* **60,** no. 1, 161–166.

Department of Geophysics
Stanford University
397 Panama Mall
Stanford, California 94305
mdenolle@stanford.edu
edunham@stanford.edu
beroza@stanford.edu

Manuscript received 25 June 2011